Meas. Sci. Technol. **19** (2008) 055601 (18pp) doi:10.1088/0957-0233/19/5/055601

Quantitative drop spectroscopy using the drop analyser: theoretical and experimental approach for microvolume applications of non-turbid solutions

N D McMillan[1], S R P Smith[2], A C Bertho[1], D Morrin[1], M O'Neill[3], K Tiernan[4], J Hammond[5], N Barnett[6], P Pringuet[1], E O'Mongain[7], B O'Rourke[1], S Riedel[4], M Neill[8], A Augousti[9], N Wüstneck[10], R Wüstneck[11], D D G McMillan[12], F Colin[13], P Hennerbert[13], G Pottecher[13] and D Kennedy[3]

[1] Institute of Technology Carlow, Kilkenny Road, Carlow, Ireland
[2] Physics Department, University of Essex, Wivenhoe Park, Colchester, Essex CO4 3SQ, UK
[3] Carl Stuart Ltd, Whitestown Business Park, Tallaght, Dublin 24, Ireland
[4] Dublin Institute of Technology, Dublin, Ireland
[5] Starna Scientific Ltd, 52–53 Fowler Road, Hainault, Essex IG6 3UT, UK
[6] Ocean Optics Ltd, Ocean Optics BV, Geograaf 24, 6921 EW Duiven, The Netherlands
[7] Physics Department, University College Dublin, Belfield, Dublin 4, Ireland
[8] Water Laboratories, Environmental Protection Agency, The Butts, Kilkenny, Ireland
[9] Faculty of Science, Kingston University, Surrey KT1 2EE, UK
[10] Anaesthesiology, Charite, Humboldt University, Berlin, Germany
[11] Institute of Physics, University of Potsdam, Potsdam, Germany
[12] TMS Consultants, Pery Square, Limerick, Ireland
[13] IRH Environnement, BP 286, 11 bis Rue Gabriel Péri, F-54515 Vandoeuvre-les-Nancy Cedex, France

E-mail: norman.mcmillan@itcarlow.ie

Received 8 August 2007, in final form 21 January 2008
Published 19 March 2008
Online at stacks.iop.org/MST/19/055601

Abstract

The drop analyser, also termed the tensiograph, is an optical fibre-based instrument system for monitoring liquids. A comprehensive assessment of the drop analyser used as a UV–visible spectrophotometer has been undertaken employing both experimental and theoretical studies. A model of the tensiograph signal (tensiotrace) has been developed using a ray-tracing approach to accurately predict the form of the tensiotrace as an aid to drop spectroscopy. An analytical equation is derived for quantitative drop spectroscopy and the form of the equation has been experimentally tested. The equation applies to both the case of a growing drop and the situation in which the drop volume is held stationary. Measurements on both stationary and moving drops are of practical value. Modelling has been used to compute the average path length of the coupled light in the drop to give a result that compares favourably with values obtained from experimental measurements. An optimized method has been identified for quantitative drop spectroscopy measurements. Results from UV–visible studies on both pollutants in water and pharmaceuticals demonstrate the utility of this approach. Two key matters relating to the practicalities of drop spectroscopy are then discussed. Some experimental studies have been made to ascertain the practical limit in analyte concentration above which variations in transmitted light from the drop shape variations result. Here, tabulated information on a representative range of liquid types has been provided as a guide to optimized spectroscopic drop analysis. Secondly, the handling of micro-volume

samples is discussed. The paper concludes with a brief evaluation of the usefulness of this drop spectroscopy approach, but specifically points to the importance of drop spectroscopy for nanoscience applications.

Keywords: drop, analyser, liquid, UV–visible, spectroscopy, colour, water, monitoring, modelling, Laplace, ray tracing, pharmaceutical, tensiography, nanoscience

(Some figures in this article are in colour only in the electronic version)

This paper is dedicated to the memory of James Bruce Stokes (1943–2007) who was an original promoter of optical drop science from 1987. Jim was a truly inspired teacher who pioneered physics and instrumentation programmes in Ireland's third-level colleges through his work initially in Sligo and then subsequently in Waterford. He was a friend and personal inspiration to Norman McMillan, in their joint work in establishing some of the first Regional Technical College programmes in the physics and instrumentation areas from 1972 onwards.

1. Introduction

The optical tensiograph, referred to here generally as a drop analyser, is an amplitude-modulated fibre optic sensor (AMFOS) instrument that provides measurements from the recording of a graphical recording known as a tensiotrace. The tensiotrace is an evolutionary signal recorded from the light coupled between a source and collector fibre as the drop moves through its entire volume-life cycle, from a remnant drop to a fully evolved drop that finally detaches from the optrode head. Full details of the instrument are given below, but here it may be helpful to explain that the tensiotrace in effect comprises a sequential recording of what are a series of internal rainbow-reflection orders second, third, etc, couplings, each associated with a distinct tensiopeak in the signal that develops at specific drop volumes. The instrument has been engineered to deliver measurements of the physical properties of the liquid under test (hereafter LUT), namely surface tension/density ratio (shape factor in drops), refractive index, colour and turbidity. The technique has been developed to provide a range of other application measurements, but most importantly, is used for fingerprinting/quality assurance of products such as beer, wines, water, petrochemical and indeed a wide range of liquids. The instrument can also be used for quality assurance (hereafter QA) for solids such as pharmaceutical products when these are dissolved in an appropriate solvent. A review of the drop analyser applications has been undertaken and spectroscopically it has uses in the sensitive monitoring in a number of water, beverage, chemical and biochemical processes [1].

The possible use of the drop analyser as a spectro-analyser is something that has for long been known [2], but there are a number of important theoretical issues that surround the use of the drop analyser as a spectrometer. None of these theoretical and practical issues that are dealt with in this study have previously been systematically investigated. The body of this paper provides the first comprehensive investigation of liquid drop UV–visible spectroscopy. Tensiotraces have been modelled using a ray-tracing approach with the drop shape theoretically defined using the Laplace–Young equation. This modelling is used to provide the theoretical basis of drop spectroscopy. Importantly, quantitatively a modified Beer's law relationship is obtained that provides a description of the observed photometric experimental measurements. This simple analytical equation adds a correction term to what is otherwise the well-known Beer's law relationship. The equation accounts for the 'differential' attenuation of rays in the 'drop cuvette' arising from the 'differential' absorption of ray paths of varying length. The simple second-order correction term involves the average path length and variance in the path length arising from the multiple coupling paths in the drop. Some discussion is made of the wavelength and volume dependences in this analytical relationship arising from this ray-tracing model. This issue is of some practical importance because there are various options for undertaking quantitative measurements with the drop analyser. A supporting experimental study is reported based on comparative measurements in two archetypical application areas. This study experimentally validates the theoretical description presented in this study. The first experimental illustration of quantitative drop spectroscopy presented is for pharmaceutical science with measurements on acetaminophen. The second study relates to water science measurement for a typical priority pollutant, namely naphthalene, with measurements of the pollutant in real waters. These two application studies are focused on comparing the respective measurement capabilities of the drop analyser to the standard UV–visible spectrophotometer. The calibration curve for the quantitative drop analyser approximates to a Beer's law measurements, but these studies show this deviates slightly from the linear at higher concentrations. The analytical relationship is found to fit accurately the experimental data.

The modelling work is used to determine the average path length and variance in the path length. The modelling average path length has been checked against those obtained experimentally. The ray-tracing and drop modelling techniques have been used to compute the average path length computed from the weighted average of all the path lengths giving consideration to the absorption of each path length for the photons reflected within the drop as they couple between the source and collector fibres. The experimental estimations of these quantities are made from a calibration study and these measurements also allow for the determination of the molar absorptivities of coloured solutions to test the analytical theory of drop spectroscopy. Drop modelling results were found to be in good agreement with the experimental

measurement and illustrate the fact that for simple solutions, analyte concentration result in relatively small changes to drop shape and hence EPL. There are differences of course between a physical 1 cm cuvette and a 'drop cuvette'. The consequences of this distribution of lengths of the coupled rays have been explored both theoretically and experimentally. It is shown that the drop spectrometer does have a very well defined and surprisingly an average path length that can be considered as a constant for low concentration measurements, which are of course the type of solutions used in the vast majority of practical chemical assays, while there is a small correction term for strong analyte concentrations.

Consideration of the physics of the drop systems suggests that advantages in calibration and analytical sensitivity (calibration sensitivity is the slope m of the measurand–measurement graph (A_T versus concentration graph in the present work) while analytical sensitivity is this value divided by the standard deviation in the measurand A_T and equals m/σ_{A_T}) of the drop detection system over the traditional UV–visible spectrophotometer could be explained in part from micro-errors in the mechanical setting reproducibility of the traditional UV–visible spectrophotometer. The real point, however, is that this type of drophead can be modified either to work as a pendant or sessile drop system. The path length can be easily varied from about 15 mm to about 1 mm, simply by scaling the head design. This of course means in practice, that the sensitivity can be adjusted by scaling and variation of the measurement drop volume. It is found possible to adjust the drophead dimensions such that the sensitivity is the equivalent of a standard spectrometer (measuring sensitively in the dynamic range 0–3 A units), but this sensitivity can be decreased by reducing the path length to enable measurements of very concentrated solutions with an absorbance up to 60 A units [3]. The enormous practical advantage of this should not be underestimated. Simply by suitable drophead scaling and/or variation of the measurement volume of the drops of LUT on a solution can be undertaken without any sample dilutions.

The present work, therefore, has for the first time provided an analytical theory of drop spectroscopy. In all other microvolume spectrophotometers no theoretical basis exists for the measurement, which provides empirical values from calibration solutions. Quantitative accuracy for the analytical theory is obtained by modelling studies which delivers from the drop physics numerical values for the constants for this analytical relationship. The model used for the pendant drop is explained as this provides the theoretical platform for this study together with the ray-tracing model that has been developed and qualitatively and numerically tested for predicting the form of the tensiotrace. The rays coupling from the source to the collector fibre are at each stage in the drop growth used to compute the photometric signal to generate the tensiotrace. The constants in the analytical theory are a function of the absorption of the LUT and relate to the average path length of the test solution and the variance in this average path length. However, the second-order drop absorbance equation approximates in nearly all practical situations to a simple linear Beer's law-type relationship. The accuracy of this small correction term has been tested in two rather 'extreme' practical measurement situations where deviations from linearity have been observed. These experimental measurements have been used to confirm the theory. The theory has been tested on large pendant dropheads of 9 mm diameter that support drops of over 100 μL. The theory does apply in general to both sessile and pendant drops, with millimetre head diameters producing average path lengths of a little over a millimetre. Such drop spectroscopy methods would be used in nanoscience with drop volumes of as little as 700 nL. Finally, the detection limits for a drop spectrometer have been experimentally investigated and the technique has been shown in a very major water pollution study to be capable of delivering results of detection limits that are of practical value. Also, the method has been tested both quantitatively and qualitatively with success in some pharmaceutical applications.

The issue of the best approach to absorbance measurement is given detailed theoretical consideration. In addition, the issues arising in drop spectroscopy using more complex test solutions in which the average path length varies due to drop-shape changes have been experimentally evaluated. Some experimental studies have been made to ascertain the variation in transmitted light in a representative range of liquid types that result from the drop shape variations. It would of course be desirable if the 'drop cuvette' were not subject to such variation during a spectroscopic analysis. The analysis of such solutions where drop-shape changes can occur, however, is simply handled in practice and although there is then a nonlinear calibration, nevertheless the measurement is accurate and furthermore represented precisely by an analytical equation. In such situations, the concentration error is not constant and will increase along the calibration curve. The scope and limitation of this experimental approach is considered. The experimental problems of using drop spectroscopy for measurements of turbid solutions are pointed out as delivery through capillary tubing to the measurement head gives rise to the SPLITS effect [4], which severely limits the performance of the drop spectroscopy approach for turbid liquids.

2. Apparatus and fundamentals of the approach

Perhaps the simplest arrangement for optical drop analyser is based on a concave drophead used in this study. This arrangement is shown in figure 1. Light from a tungsten or LED source is injected into the drop through the source fibre. The drophead employs standard 1 mm polymer or silica fibres, which are polished using 0.3 μm diamond paper before being glued into the drophead. The head diameter is 9 mm; the fibres are 6 mm apart and the ends are left protruding a slight distance from the concave base. The head diameter is critical to ensure that all relevant features of the tensiotrace are seen. Recently, new designs of quartz head have overcome all the major problems associated with damage to the drophead that produces changes in the tensiotrace over time. The liquid is delivered via a HPLC capillary glued into the centre of the drophead. Ideally, the head should be designed such that it wets (i.e. the suspended liquid covers the entire lower surface

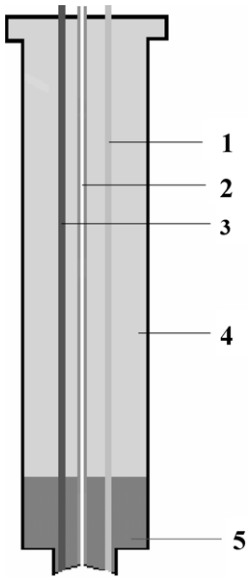

Figure 1. Drophead showing (1) source fibre, (2) liquid feed, (3) collector fibre, (4) drop cylinder and (5) concave drophead.

of the drophead). The drophead was fitted into a brass Peltier heater block and maintained usually at 25 °C (stabilization at 20 °C is quite difficult as it is too close to ambient temperature in most laboratories). Measurements were taken with various LED sources and a phototransistor detector. The optoelectronic signal was processed via a standard 16-bit resolution PIC microcontroller with the data processed using purpose-written software. Full details of the experimental set-up can be found elsewhere [5]. The instrument can be fitted with various Ocean Optics hardware such as their pulsed xenon, deuterium CW and high-power xenon sources working with any of their CCD detector systems. The system currently uses a UV-enhanced configuration from Ocean Optics Inc. (USB2000 with holographic grating 1800 mm^{-1}, 200 μm slit, detector lens and UV detector upgrade covering the wavelength range from 200 nm to 415 nm).

The signal is picked up by the collector fibre and delivered to a phototransistor/photodiode or CCD detector. The instrument records a single signature trace, called the 'tensiotrace', which is scissored from the incoming A/D detector signal. The tensiotrace is obtained from recording the optoelectronic signal between the falling of two drops from the head. Data acquisition begins when a 'trigger drop' falls from the drophead between a pair of optoelectronic 'eyes' situated below the drophead. The signal is recorded until the second drop, the 'measurement drop', falls. The signal is then converted to digital form by an A/D card and the resulting tensiotrace is stored in the computer archive system.

A steady drop growth tensiotrace obtained for pure water is illustrated in figure 2. The principal features of the separation vibration (label 1 in figure 2), first-order protopeak (label 2 in figure 2) that does not couple via TIR reflections in the standard drophead, but has been observed in other drophead designs, the second-order rainbow peak (label 3 in figure 2) which provides two good measurands for tensiotrace

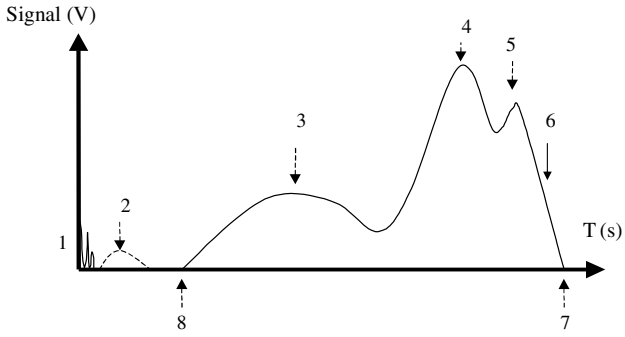

Figure 2. Tensiotrace showing the important trace features labelled 1–8 as follows: (1) separation vibration; (2) first-order peak (protopeak); (3) rainbow (second-order peak deuteropeak); (4) tensiopeak (third-order tritopeak); (5) shoulder peak (fourth-order tetartopeak); (6) separation peak (fifth-order pemptopeak); (7) drop period; (8) rainbow peak commencement.

analysis the peak period t_2 and peak height h_2, the third-order tensiopeak (label 4 in figure 2) which also provides two good measurands the peak period t_3 and peak height h_3 and finally the fourth-order shoulder-peak (label 5 in figure 2) which can give in some tensiotraces two further measurands the peak period t_4 and peak height h_4. There are other very useful measurands to be obtained from the tensiotrace, namely tensiotrace period (label 7 in figure 2) and the rainbow commencement (label 8 in figure 2). The latter measurand has demonstrated very good measurement potential for surface tension measurements. The tensiotrace period (t_3) of course corresponds to the same measurement parameter tensiotrace period (T_1) that is the measurand basis of the science of tensiometry and the classical Harkins and Brown [6] method of surface tension measurement. Recently, the empirical basis of this method has been put on a theoretical foundation by Basaran and co-workers [7]. It has been found in a general and wide-ranging study that there is a linear relationship between this tensiotrace period and tensiograph peak period. There exists a simple empirical relationship

$$T_1 = \zeta t_3 \text{ and } \zeta' t_3 \tag{1}$$

where ζ and ζ' are two dimensionless constants known as the 'fundamental tensiometric constants'. It has been experimentally demonstrated that there exist only two linear relationships between T_1 and t_3. A bifurcated relationship exists as salts lie on a line of their own with slope ζ' and all other liquids on a line with slope ζ. The fulcrum data point is water. This discovery of the heretofore relationship clearly has very major implications and will not surprisingly be the subject of a future paper devoted exclusively to this and other new relationships that exist between the various tensiotrace measurands [8].

Various features can be used as measurands to obtain measurements of various physical and chemical properties of liquids with the drop analyser. Tiernan, Kennedy and McMillan give details of the performance of this earlier generation of tensiograph [9]. Details of how these measurements are obtained have been recently reported elsewhere [9], based on updating the earlier work of

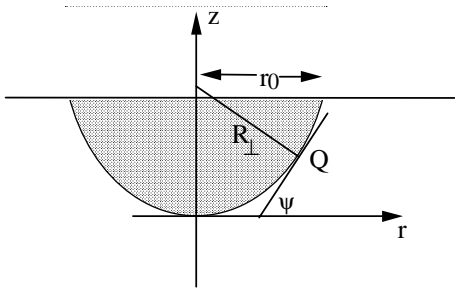

Figure 3. Schematic representation of a hanging drop held up by surface tension.

McMillan [10]. The rainbow peak height gives very sensitive measurement possibilities for refractive index of the LUT, the tensiopeak height similarly for colour. Both peaks show sensitivity to the two properties of the LUT, but exhibit very strong specificity, if not completely overwhelming dependence, on the one property (refractive index for rainbow and colour/turbidity for tensiopeak). Recent work by Tiernan has given an explanation of these dependences [11]. The drophead engineering has sought to maximize these specificities. Independent measurement of both physical quantities are relatively straightforward in all circumstances given calibration data are available. The structure of the separation vibration has been studied with a view to obtaining measurements of surface tension from the frequency of remnant drop vibration and viscosity of the LUT from the damping in this vibration [12].

3. Theory and modelling

3.1. Drop equations

The modelling of drops is done using the classical Laplace–Young equation that is used to reconstruct the shape of a hanging drop held up by surface tension as shown in figure 3. The drop has radius r_0 at its top, where it is attached to the drophead. At a point Q on its surface (radius r, height z above the bottom of the drop), there is a pressure difference Δp between the inside and the outside of the drop, which is balanced by a surface tension force

$$\Delta p = p(\text{inside}) - p(\text{outside}) = \left[\frac{1}{R_\perp} + \frac{1}{R_\parallel}\right], \qquad (2)$$

where $R_\perp$ and $R_\parallel$ are, respectively, the radii of curvature out of plane and in plane at Q. A theoretical model has been developed of drop shape using Runge–Kutta fits.

In the numerical solution of the above equations, there are two parameters, β and X_0, where

$$X_0 = \frac{r_0}{R_0}; \qquad \beta = \frac{\rho g r_0^2}{2T}. \qquad (3)$$

β is determined by the properties of the liquid under investigation, and has typical values in the range 1–5 for the drophead radius r_0 used in our measurements. X_0 on the other hand must be varied in order to simulate the increasing drop volume. $X_0 = 0$ corresponds to a small drop that is flat ($R_0 \to \infty$) at its base; as X_0 increases, the drop volume V increases, though there is no simple relationship between V and X_0. Eventually, the drop volume reaches a maximum with increasing X_0; beyond this point the drop will not stable and so it detaches itself from the drophead.

Figure 4 shows the results of the Laplace–Young modelling. All drops are physically realizable because they are described by this physics. In the figure there is shown a series of modelled drop shapes from the smallest physically realizable remnant drop to the largest physically realizable drop.

3.2. Modelling tensiotraces

A computer program has been written that simulates the response of the drop analyser using a ray-tracing procedure. The passage of a cone of rays from the source fibre comprising at least 1000 rays (20 000 is more typical) is followed through the liquid, taking account of reflections at the supported pendant drop surface. If the ray eventually strikes the detector fibre within the acceptance angle of the fibre, its intensity is added to the total. The model allows for the reflection coefficient at the drop surface (which depends on the refractive index), and can also include the effects of absorption. Drop shapes are generated between the smallest realizable physical drop that conforms to the Laplace equation (remnant drop) and then the largest drop that can be maintained on the specific drophead. The drop separation volume is identified in the modeling as a physically impossible point; an incremental increase in the volume is modelled, but the resulting drop volume decreases. The emission from the multimode fibre is modelled by a cone of rays from the source fibre that are followed through the liquid, taking account of reflections at the surface of the drop. The intensity distribution from the fibre uses the approximation of a simple $\cos^2\theta$-dependence. If the ray eventually strikes the detector fibre within the acceptance angle of the fibre, its intensity is added to the total. The rays are subject in the passage in the drop to attenuation from absorption based on the length of the ray that couples between source and collector fibre. Rays are traced around the inside of the drop and obviously obey the simple law of reflection given the Fresnel reflection coefficient for the angle of incidence of the ray and the drop surface.

Typical results are shown in figure 5. The total reflectivity (continuous curve) includes all contributions. The individual curves show the contributions from rays that undergo two, three and four reflections at the drop surface (there is no contribution from single reflections); these curves are simple ray counts, and do not include losses on reflection at the drop surface. The full ray-tracing tensiotrace model, however, does of course include computation of all losses.

The 3D ray-tracing results reveal the nature of the reflection processes that lead to the rainbow and tensiopeak couplings. Results obtained from ray-tracing calculations by Smith show the extreme sensitivity to the positions of the source and detector fibres, illustrating the need for precision construction of the instrument if reproducible results are to be obtained.

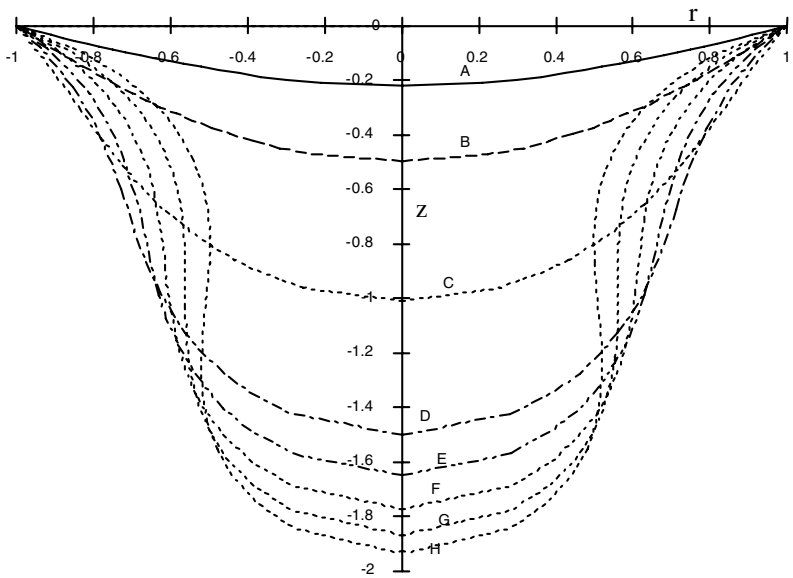

Figure 4. Typical drop shapes for water, where the curves A−H are for increasing X_0 until the drop detaches at H.

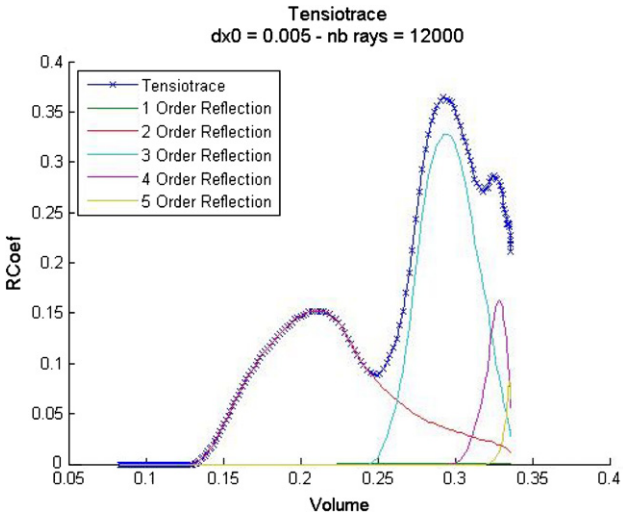

Figure 5. Typical results obtained from ray-tracing calculations. Modelling results show that the rainbow peak is uniquely formed by the two reflections rays, the tensiopeak is composed of three reflections rays, while four and more simultaneously coupled reflections comprise the shoulder peak.

3.3. Drop analyser absorption theory

In the drop analyser, the situation is unfortunately more complex than in the standard spectrophotometer, where it is assumed that given good collimation, all path lengths are identical and the absorbance (A) of the LUT is obtained using the well-known standard photometric measurement procedure. In a drop spectrometer, there are various options for measurement. The average path length in drop spectroscopy increases as the volume increases, and even for a drop of fixed size there is a range of paths of different lengths for the light going from source fibre to detector fibre. It is therefore important to distinguish between the drop analyser and UV–visible absorbance and therefore a subscript will be used to designate the former measurement (A_T). For measurements taken from a single tensiotrace point the formulation originally proposed by McMillan [13] holds

$$A_T = \log_{10} \frac{\langle V_{0i} \rangle}{\langle V_{tj} \rangle} \quad (0 < A_T), \tag{4}$$

where $\langle V_{0i} \rangle$ is the average height of the tensiopeak (data point i) for the blank measured in volts and $\langle V_{tj} \rangle$ is the average height of the same peak (data point j) for the sample measured in volts.

In the usual measurement situation at the peak maxima it is clear that $i \cong j$, as is found in nearly all measurement situations with low-concentration analytes in which reference and test liquids have approximately the same tensiotrace period (T_1), that peak measurement positions would be identical within limits of normal measurement reproducibilities. There are two important measurement options. The first practical situation is when the spectroscopic measurement data are taken using the appropriate peak data derived from the series of temporal tensiotrace data samples. The second situation is when the pump is programmed to stop at the peak maxima and then CCD or CMOS camera averaging is used. Increasing the integration time of the CCD enables the measurement accuracy of these height measurements to be improved by the usual experimental averaging procedures. These two distinct approaches will be called, respectively, the dynamic and static spectroscopic quantitative modes, but both will use equation (4) to calculate the tensiograph absorbance (A_T).

The drop spectrometer is an instrument that delivers a voltage output measured against the volume of liquid delivered, which of course, relates when using a computer-controlled stepper pump delivery directly to time of liquid delivery. This voltage is quantified from an A/D conversion in a custom circuit when the instrument is operating via LED sources, or alternatively via the A/D in a CCD detector circuit.

In both cases the voltage represents stored or dynamic charge derived from the photon flux in the detector fibre.

The absorption produced by the chromophore is, however, encoded throughout the entire tensiotrace. There are therefore other options for absorbance measurements based on using the entire data from the tensiotrace. A number of measurement options for obtaining the absorbance of the LUT using the entire data in the tensiotrace have been investigated but in all cases these gave a greater experimental error than either of the dynamic or static spectroscopic modes. These modes of course have the added virtue of being both elegantly simple to understand and easy to implement. It is perhaps worth just expanding briefly on this statistical study that will not be fully detailed here given that this delivered a negative result. Reiterating, all the digitized points in the tensiotrace, with the exception of those in the noise or below the detection limit, contain useful information about molar absorptivity of the LUT. Clearly, the tensiotrace absorption encoding is complex and the calibration sensitivity (slope of the graph) of measurement varies at each digitized (temporal) measurement position in the tensiotrace. The issue to be resolved in the first instance surrounds the optimum statistical averaging procedure that can be employed to compute the absorbance from the entire tensiotrace data set. A number of different statistical methods (straight average, weighted-average using signal magnitude for weightings and information average using $\log_2$[signal/noise] to weight the data) of taking measurements from the entire tensiotrace signal have been considered. All these methods have been tested for their efficacy in absorbance measurement with experimental studies. The results of this long study has shown conclusively that the best method is simply to use the static spectroscopic mode since this measurement at the signal maxima (peak position) with signal averaging produced the optimum result. CCD or CMOS system of course averages in time and from the multi-spectral data set captured many tensiotraces at various wavelengths for the look-up-table (LUT) can be simultaneously generated. Averaging is here therefore used in the traditional way to determine the result with the standard deviation used to determine the experimental error.

The way in which a tensiotrace changes with increasing absorption in the LUT is complex and certainly subtler than in a standard optical absorption measurement. In this case, the optical effective path length is not a fixed parameter of the system. In the standard type of optical absorption measurement, the light passes through a fixed effective path length ℓ. The relative optical intensity due to absorption along a path of length ℓ is

$$R = \exp\{-\alpha \ell c\}, \tag{5a}$$

where α is the absorption coefficient of the optical material.

The effect of turbidity is more complicated. We have used the following procedure to simulate the effect. Under turbid conditions, the direct ray suffers a loss of intensity over a path ℓ similar to the loss due to absorption,

$$I = I_0[1 - \exp\{-\alpha_T \ell\}], \tag{5b}$$

where α_{T} is the turbidity scattering coefficient. However, the intensity $I_0 \exp\{-\alpha_T \ell\}$ removed from the direct ray is not absorbed, but contributes to a turbidity-generated optical energy density within the liquid drop. We assume that this energy density is in the form of isotropic radiation, which escapes from the drop at its air surface and also escapes into the drophead. Some of the latter radiation will find its way into the exit fibre, and will be detected as indirect turbidity-scattered light in addition to the light detected by the direct rays. The calculation of the effect of turbidity is straightforward, given these assumptions, but the details are too lengthy to be specified in this paper, but it is perhaps important to point out that similar measurement approaches can be developed for turbid solutions as to those set out below for absorbing solutions.

The optical absorbance A is defined by $A = -\log_{10}\{R\}$, so

$$A = \log_{10}(e)\alpha \ell c = 0.4343\,\alpha \ell = \varepsilon c \ell. \tag{6}$$

This is the well-known Beer–Lambert law, stating that A is linearly proportional to the path length (ℓ). Here, α is the absorption coefficient, ε is the molar absorptivity and c is the molar concentration.

Suppose a beam of light passes through an absorbing material in such a way that there is a range of paths from source to detector. Let the probability that the path length lies in the range ℓ to $\ell + \mathrm{d}\ell$ be $P(\ell)\,\mathrm{d}\ell$, normalized such that $\int P(\ell)\,\mathrm{d}\ell = 1$. The EPL (effective path length) can be defined from equation (5) as

$$\ell_{\mathrm{eff}} = A/\varepsilon c \tag{7a}$$

and in the specific case of the drop analyser

$$\ell_{\mathrm{eff}} = A_T/\varepsilon c = \ell_1 - 1.152\,78\,\varepsilon c\,\Delta\ell^2. \tag{7b}$$

It should be noted that ℓ_{eff} and ℓ_1 are different things,

$$\ell_1 = \int \ell\, P(\ell)\,\mathrm{d}\ell. \tag{8}$$

The overall relative absorption factor is therefore given by the quantity

$$R = \int \exp\{-\alpha \ell c\} P(\ell)\,\mathrm{d}\ell. \tag{9}$$

Clearly, the absorbance $A = -\log_{10}\{R\}$ is now not simply equal to $\varepsilon c \ell_1$. One can perform an expansion valid for weak absorption in order to see the size of this effect. To second order in α,

$$\begin{aligned} R &\approx \int \left\{1 - \alpha \ell c + \frac{1}{2}\alpha^2 \ell^2 c^2\right\} P(\ell)\,\mathrm{d}\ell \\ &= 1 - \alpha \ell_1 c + \frac{1}{2}\alpha^2 \ell_2^2 c^2, \end{aligned} \tag{10}$$

where ℓ_2 is the rms path length defined as $\ell_2^2 = \int \ell^2 P(\ell)\,\mathrm{d}\ell$. Then

$$\begin{aligned} A_T = -\log_{10}\{R\} &\approx 0.4343\left[\alpha \ell_1 c - \tfrac{1}{2}\alpha^2 c^2\left(\ell_2^2 - \ell_1^2\right)\right] \\ A_T &= 0.4343\alpha \ell_1 c - 0.217\,15\alpha^2 c^2\,\Delta\ell^2. \end{aligned} \tag{11a}$$

In terms of the molar absorptivity, which is the usual formulation employed in chemistry:

$$\begin{aligned} A_T &= \varepsilon c \ell_1 - \varepsilon^2 c^2\,\Delta\ell^2/(2 \times 0.4343) \\ A_T &= \varepsilon c \ell_1 - 1.152\,78\,\varepsilon^2 c^2\,\Delta\ell^2. \end{aligned} \tag{11b}$$

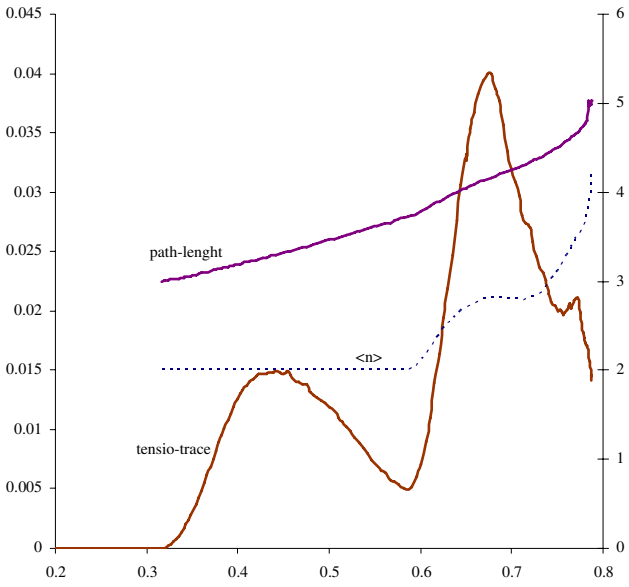

Figure 6. Modelling results, showing tensiotrace (LH scale), and (RH scale) normalized EPL path length and average number of reflections, plotted as functions of normalized drop volume. Average path length (ℓ_1) (upper curve) and variance ($\Delta\ell^2$) (lower curve) as functions of drop volume modelled for water on a 9 mm drophead.

This result is one of considerable analytical importance to drop spectroscopy and shows that, for small absorption, the optical absorbance falls below the linear Beer's law by an amount proportional to the variance

$$\Delta\ell^2 = \ell_2^2 - \ell_1^2. \tag{12}$$

Of course, if the measurement involves only a single determination of ℓ_1, then the Beer's law approximation applies and $\ell_2 = \ell_1$.

It is perhaps worth here just giving some more thought to this correction factor and its relation to the form of what we might call the drop spectroscopy Beer's law relationship. Common sense would immediately suggest that if drop shapes of the LUT were essentially unchanged, as is indeed the case in the usual practical working situation, when analysing a set of very dilute concentrations of analyte, then both (ℓ_1) and the variance ($\Delta\ell^2$) are in essence just a quantifiable function of the absorbance of the test liquid.

Figure 6 is important as it quantifies the variation in both the average path length (ℓ_1) and the variance. It is important to say that in water the tensiopeak occurs at a volume of 0.3 on this diagram. We see that as the drop grows in volume the average path length increases in an approximately parabolic fashion until close to the drop separation. The average path length varies between 0.8 cm and 1.8 cm (approximately two and four times r_0). The variance is extremely small until third-order reflections come into operation when a variance of around 0.0015 is obtained. The variance increases in a radical way at this point which is really an anomaly arising from the fact that just at the end of the drop cycle we observe somewhat paradoxically that a very strong first-order reflections develops. These rays have a shorter path length than rays with 2, 3 or more reflections and thus increase the variance. This is not a problem in practice because the drop separates from the head having reaching its maximum volume probably because of the smallest perturbation due to vibrations.

Figure 7 shows a graph of ℓ_1 and the variance $\Delta\ell^2$ plotted at each point as an error bar with absorbance of the LUT in the range $A = 0$–3.5. This modelling yields the average path length as

$$\ell_1 = -0.0132A_T + 1.377. \tag{13}$$

It is clear from this figure that the variance in the path length, which is of course calculated from the model is almost constant and has a value of $\Delta\ell^2 = 0.0021$. Tensiotraces of water and dye solutions have modelled assuming that the analyte does not change in a measurable way the other physical properties of the

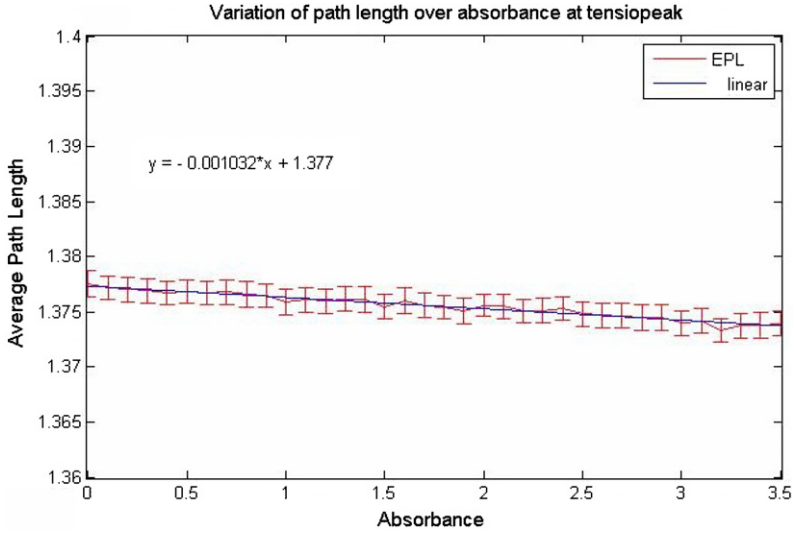

Figure 7. Modelled variation in the average path length and variance in the path length in a water drop on a 9 mm diameter head for absorbance values 0–3 A units.

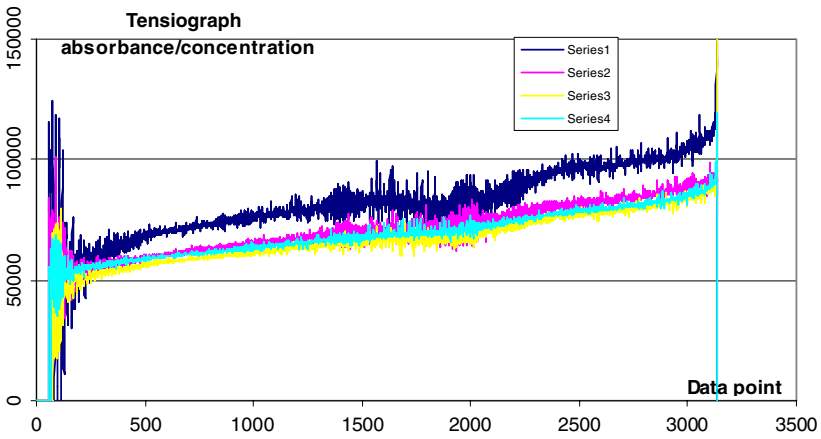

Figure 8. Plot of A_T/c ($=\varepsilon \times \ell_{\text{eff}}$) plotted against volume (data point) for blue dye for solutions. The plots are for four concentrations 1.29 μM (Ser 1), 2.5 μM (Ser 2), 3.77 μM (Ser 3) and 6.25 μM (Ser 4). The x-axis is drop volume, 3000 corresponding to approximately 90 μL.

water. This is found in practice to be a very accurate modelling assumption. Absorbance values have been modelled for the range 0–3.5 as this is the usual spectroscopic range for standard instruments. The measurement at a peak is always made somewhat problematic because of noise effects the value in the most critical way at such a point of inflexion. The path length at the tensiopeak is plotted against absorbance to show that the path length does not change at a given volume.

The graph, as theoretically predicted, has a slight negative slope as the path length is shortened with absorbance. The cause for this foreshortening of the average path length being simply that attenuation of various path lengths inside the drop is greater for the longer than the shorter paths. It should also be noted that the slope on this graph is only visible due to the zoom factor used. Both the slope and variance shown by the error bars at each of the modelled absorbance positions are very small.

This result shows that the tensiography is capable of measuring absorbance from results taken at the tensiopeak position and this to a very good approximation will be a simple Beer's law relationship.

The modelling shows that the average path length and its variance are quantifiable numbers so an exact relationship including the very small analytical correction can be obtained for equation (11). It is clear, however, that the equation we have for drop spectroscopy devolves to one with circular form, in that the measured tensiograph absorbance appears on either side of the equation. Numerical methods can, however, be used to solve this second-order equation in concentration,

$$A_T = 0.4343\alpha(-0.0132A_T + 13.77)c - 0.004\,48\alpha^2c^2, \quad (14)$$

$$A_T = \varepsilon c(-0.0132A_T + 13.77) - 0.002\,38\varepsilon^2c^2. \quad (15)$$

The general approach would be then to take ratio measurements of absorbance at corresponding positions (volumes) in the tensiotrace from a measurement and blank drop. There are a series of tensiotraces recorded at each wavelength (λ) and each wavelength in general will present a different tensiotrace to the next if there is an absorbing species present in the LUT. It is perhaps best to give the analytical relationship for tensiographic absorbance $A_T(\lambda, V)$ showing the functional dependences for the dynamic quantitative measurement mode. The dependences are given here in italic were λ is the wavelength in nm, V is any selected volume of the drop measured in μL and A is the absorptivity of the liquid measured using a standard UV–visible measured in A-units. For measurements taken on the growing drop in a dynamic mode then the volume is a continuously changing variable

$$A_T(\lambda, V) = \varepsilon(\lambda)\, c\ell_1(A, V) - 1.151\,28\varepsilon(\lambda)^2\Delta\ell^2(A, V)c^2 \quad (16a)$$

but at the tensiopeak position the modelling tells us that

$$A_T(\lambda, V) = \varepsilon(\lambda)c\,(-0.0132A_T + 13.77) - 0.002\,42\varepsilon(\lambda)^2c^2. \quad (16b)$$

For the static quantitative mode when the pump is stopped the volume is fixed. The reflection inside the drop is here maximized given that the pump is stopped at the rainbow peak. This measurement approach offers a simplified situation:

$$A_T(\lambda) = \varepsilon(\lambda)c\ell_1(A) - 1.151\,278\varepsilon(\lambda)^2\Delta\ell^2(A)c^2 \quad (17a)$$

$$A_T(\lambda) = \varepsilon(\lambda)c\,(-0.0132A_T + 13.77) - 0.002\,42\varepsilon(\lambda)^2c^2. \quad (17b)$$

Equation (16) applies for the dynamic spectroscopic quantitative mode, while equation (17) applies for the static spectroscopic quantitative mode. While it is shown that the latter gives the best measurement of absorbance, there is a practical requirement for absorbance measurements to be taken from data acquired simply as part of a routine tensiotrace measurement procedure. These formulations are also extremely important for the microvolume drop spectrometer.

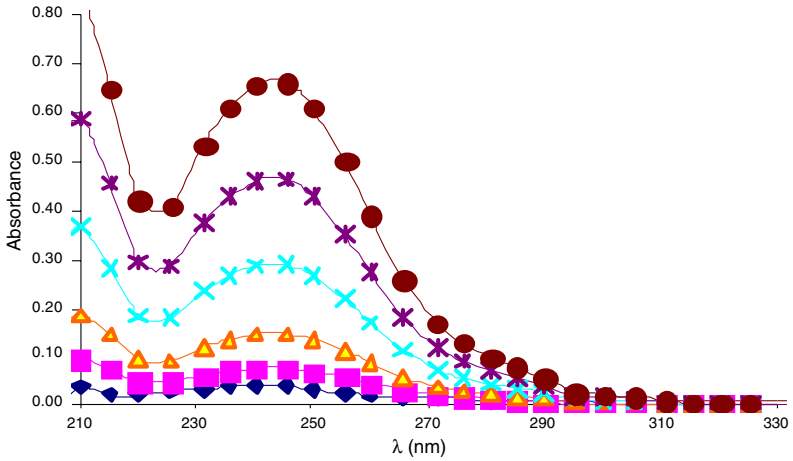

Figure 9. UV–visible spectra of acetaminophen for concentrations 625 ppb, 1250 ppb, 2500 ppb, 5000 ppb, 8000 ppb and 11 500 ppb.

4. Experimental details

4.1. Effective path length determination of drop spectroscopy

In order to determine the tensiographic absorbance, it is being assumed that the tensiograph peak maximum is in an equivalent position for each trace. Probably, the first question to ask is about how the EPL (ℓ_{eff}) varies with the concentration variation of the analyte. Here experimental determination of the drop path length has been carried out using two different methods. First of all, by comparing absorbance values obtained by UV–visible spectroscopy and tensiography assuming a simple uncorrected Beer's law approximation to obtain EPL estimates; then by using ray-tracing software developed by Smith to obtain modelled values of average path length.

The maximum tensiograph peak height has been used previously for absorbance measurements. The temporal position of these peaks may vary slightly since drop volume and drop shape vary very slightly between samples. For theoretically well-grounded absorbance reading, the average path length of light coupling to the source from the detector fibre should be identical in both reference and test measurements. Clearly, this is not possible in an absolute way if there are any changes in the shape of the drop arising from differences in the small quantities of say the absorbing species. However, for the majority of liquids, the variation in the path length is imperceptivity small and does not cause any additional error contribution to the measurement. Some attempts have been made to below to quantify the changes in EPL arising from these variations in the LUT that are discussed below.

4.1.1. Path length determination from absorbance measurements proof of the theory. A study has been made using dilute solutions of the food colorant dye (FCF blue #1 (C.I./42096)). Figure 8 shows the results of the data analysis on the series of four concentrations of blue dye solutions. The graph shows an experimental trend closely following the features predicted in figure 6 from the drop modelling. The path length variation in figure 6 is plotted against drop volume, which is directly equivalent to the x-axis to time 'data points' because the stepper pump delivers volume uniformly with time. The y-axis is a calculation from the experimentally determined optical signal, to give a measure of effective path length in the drop. This variation can be compared directly with the average path length results from the drop modelling. Details of these test solutions are given in section 4.4 below. It was assumed that given the dilute nature of these solutions a first-order Beer's law relationship would be obtained. At each point in the tensiotrace absorbance calculations were made and the value divided by the concentration of the solution using equation (7*a*). This ratio gives an experimental measure of the effective path length × molar absorptivity of the solution. Clearly, the initial data in these graphs are unreliable as the tensiotrace was noisy in this initial period due to drop oscillations. When a drop falls from the head there is a period of damped vibration. Beyond 15 s (data point 500), however, the drop has stopped vibrating and the measurements give a reliable value of the EPL obtained. From these calculations the initial drop path length is calculated to be 9 mm, rising thereafter to 12 mm at drop volume corresponding to a time of 90 s (data point 3000). The importance of this result is that we are predicting that the EPL in all these drops should be identical, given that the concentration of food dye is so miniscule, that the drop shape of all measurement drop scans can be assumed to be identical. The results presented here indeed confirm this working hypothesis, for although the tensiotraces are markedly different (see figure 12 below) the computation produces graphs of three sets of data (Ser 2, 3 and 4) that sit within experimental error, one on top of the other. The measurement for the 1.26 μM solution (Sere 1) is, however, significantly offset from the others three lines. The displacing of this line is interpreted as arising from measurement instrumentation error due to measurements being below the instrument detection limit. This result is taken as a very good experimental proof that first-order Beer's law drop spectroscopy relationships hold for liquids in which there are very minimal variations in drop shape due to the analyte.

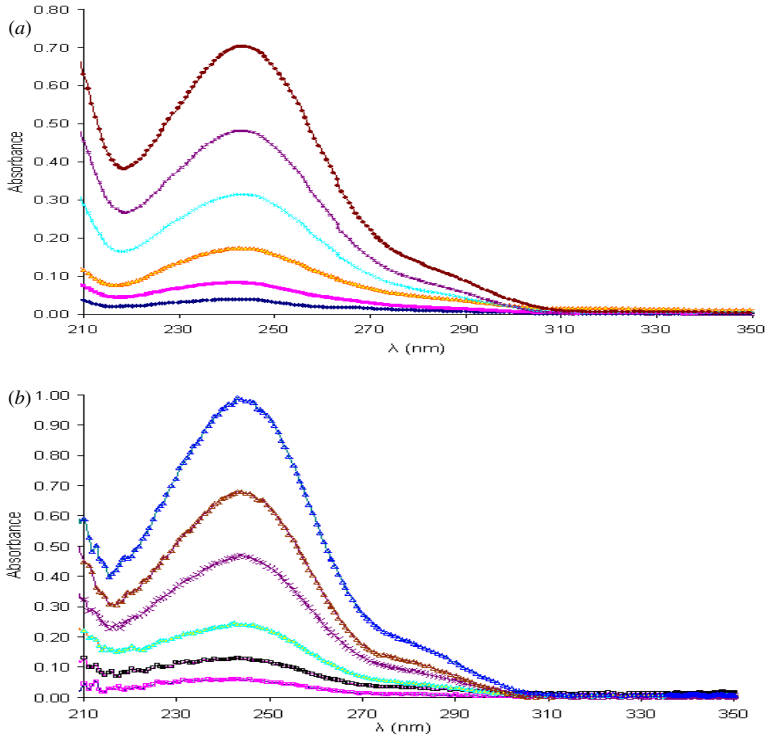

Figure 10. (*a*), (*b*) Drop spectra obtained for of acetaminophen for concentrations 625 ppb, 1250 ppb, 2500 ppb, 5000 ppb, 8000 ppb and 11 500 ppb using data obtained at the rainbow and tensiopeak positions, respectively.

Tensiotrace recording of a series of acetaminophen solutions in the range of concentrations 625 ppb, 1250 ppb, 2500 ppb, 5000 ppb, 8000 ppb and 11 500 ppb were obtained. See figures 9 and 10 for visual comparison of standard UV–visible spectrophotometer and drop analyser spectra. Interestingly, in this spectral study there is no need of a separate blank to be used as the acquisition point for the tensiotrace formed at $\lambda_{410\ \mathrm{nm}}$ as this pharmaceutical active does not absorb at this wavelength and the test sample can itself be used to provide the blank reference. In fact, light intensity at each wavelength from $\lambda_{200\ \mathrm{nm}}$ to $\lambda_{410\ \mathrm{nm}}$ were saved at each temporal acquisition point of tensiotrace formation. The position of λ_{max} was then measured with the drop analyser and found to be (242.5–243.5) $\pm$ 0.5 nm for acetaminophen measured in water in agreement with Gerhardt [14] and Clarke [15]. This study was repeated for acetaminophen with ethanol used as the solvent with a result (249–250) $\pm$ 0.5 nm that is in agreement with the standard values reported by Bayer [16] and Clarke [17]. Referencing against data from one CCD reference tensiotrace at 410 nm corresponding to the peak maxima, it was shown that the peak positions were identical for all practical purposes for all the test solutions of acetaminophen at the measurement wavelength λ_{max}. Secondly, an estimate of the EPL has been made assuming a simple approximation of an uncorrected Beer's law relationship. The standard molar absorptivity of λ_{max} for acetaminophen was taken to be 3.16×10^4 L mol^{-1} cm^{-1} for this study. The result demonstrates that for drop spectroscopy Beer Lambert law is very closely obeyed despite the fact that we know from the above theory equations (16) and (17) that there is in fact a second-order correction term in the drop spectroscopy equation. The estimated EPL remains 15 $\pm$ 0.1 mm for all the test solutions measured against the blank. This result shows impressive measurement reproducibility for all these solutions in the full range of concentrations of acetaminophen. One practical test really is all that matters fundamentally here, namely, it has been found that in a wide range of test solutions that similar impressive results, both in providing a visual match and in quantitative measurement results, the drop analyser spectral analysis matched that of the standard instrument. This finding lends the strongest practical support to the use of drop spectroscopic analysis.

4.1.2. Practical issue of path length variations for drop spectroscopy. It appears on the basis of practical investigation that variations in water drops containing non-surfactant dye molecules do not present a problem for the application of the ratio calculation to obtain the value of A_T using equation (4). The authors have found linear Beer's law-type relationships in all but a very few untypical liquid types. Most experiments used a reference blank solution (distilled water in most cases, but low-concentration admixtures of methanol for example was also used as a blank as the solvent was required to get some of the PAH compounds into solution). For other experimental studies a self-referencing situation was employed in which the sample itself is used as the blank (see section 4.1.1 where a CCD detector was employed and there are wavelengths at which the test sample does not absorb). Such

Table 1. Variation of average path lengths with concentration for a series of solutions taken from tensiographic measurements applying equation (7*a*).

	Variation in coupled light at rainbow peak	Variation in coupled light at tensiopeak
Glycerol (M)		
9.5 m	100	100
0.19	88	92
0.665	76	90
0.95	66.5	87
Di-sodium hydrogen orthophosphate dodechydrate (M)		
428 μ	100	100
48.5 m	89	94
0.188	73	89
0.285	64	87
Ammonium nitrate (M)		
9.5 μ	100	100
475 μ	95	95
9.5 m	93	94
0.19	93	96
Sucrose (M)		
9.5 μ	100	100
475 μ	109	105
9.5 m	110	105
0.19	110	105
Sodium dodecyl sulphate (M)		
95 n	100	100
9.5 μ	102	100
238 μ	80	85
713 μ	66.5	72
Sodium chloride (M)		
9.4 m	100	100
0.24	90	95
0.95	67	87
1.9	49	84

a situation must be considered as providing the ideal reference tensiotrace as this gives exactly the same drop and measured at identical conditions and time. The drop cuvette can usually be considered as closely approximating to a constant in the measurement process as the EPL will not vary from drop to drop. Linear calibrations have been repeatedly found [18]. For surfactant solutions, and indeed some other LUT, there will be an appreciable alteration in the shape of a drop. An attempt to give some rough measures on the variation in EPL that will arise in different test liquids has been made through an experimental study. Such information is clearly vital in proscribing strict limits on the range of solutions that can be measured with this technique. Table 2 gives the calculated variation in light throughput in the drop for what is hopefully a fairly representative set of solution types. These liquids have been selected as being typical of those used in the general chemical procedures. This table gives measures of throughput for varying ranges of concentration of these liquids. The effect of surface activity on drop shape is assessed in this study using the surfactant SDS.

Table 1 gives some guidance for the practical drop spectroscopist into the range of liquid types and associated concentrations that might be used to obtain optimized linear Beer's law calibrations. The variations in each case attempts to show the borderline (threshold) at which variations in transmitted light in these solutions begin to occur. For example, if we take the last chemical in the table, namely sodium chloride, then so long as solutions with concentrations below 9.4 m mol are used, then there is no practical change in light transmission path due to concentration variations in this analyte. In such a situation, photometry can be undertaken and we can anticipate that there will be a linear Beer's law-type relationship. This threshold condition is the same for both tensiograph peaks, so no variation is observed in either the rainbow or tensiopeak transmission. In practice, if dilutions are below the threshold, they would produce no measurable variation in light transmission from the presence of the analyte. It is hopefully clear to the reader that the values at the top of each of these lists of percentage variations would be a threshold below which the quantitative measurement will deteriorate. The only really troublesome chemical in this regard is the surfactant SDS, which is not at all surprising. It is very well known that water drops change shape radically for minute concentration of this surfactant.

4.2. UV-drop spectroscopy

The ultraviolet spectra of different concentrations of acetaminophen shown in figure 9 were obtained using a double beam UV–visible spectrometer at 20 °C. The purpose of including these results is for comparison purposes with the drop spectra obtained with a drop spectrometer shown in figures 10(*a*) and (*b*). These results taken on the acetaminophen sample were measured in 10% (v/v) ethanol/water. Since acetaminophen does not absorb above 330 nm the measurement requires a definition of the tensiopeak and rainbow peak periods of the reference LUT.

The experimental approach here is to obtain measurements applying the usual procedure for tensiotrace generation, but working with the Ocean CCD fibre spectrometer operating over a wavelength range of 200–410 nm. Using the same acquisition time, at the same stage of drop generation, the absorbance of each concentration of acetaminophen in 10% (v/v) ethanol/water was then obtained by applying equation (4). In these measurements, it is clear that the tensiotrace here presents for the same measurement volume of both the reference or test solutions a constant EPL to a very good approximation. Obviously, corresponding times in the CCD measurement must be used to determine the unknown concentration of the acetaminophen. The measurement assumes that the concentrations of sample do not materially change the shape of the drop and hence EPL in test and reference tensiotraces correspond to a high degree.

The spectra obtained using drop spectroscopy compare most favourably with the UV spectra obtained spectrophotometrically. The measurements of positions of λ_{max} correspond not only in these studies, but it has been found in numerous other spectra that the measurements of these peak positions can be accurately and reproducibly obtained using drop spectroscopy.

The tensiographic absorbance measurements are obtained from corresponding data acquisition time representing,

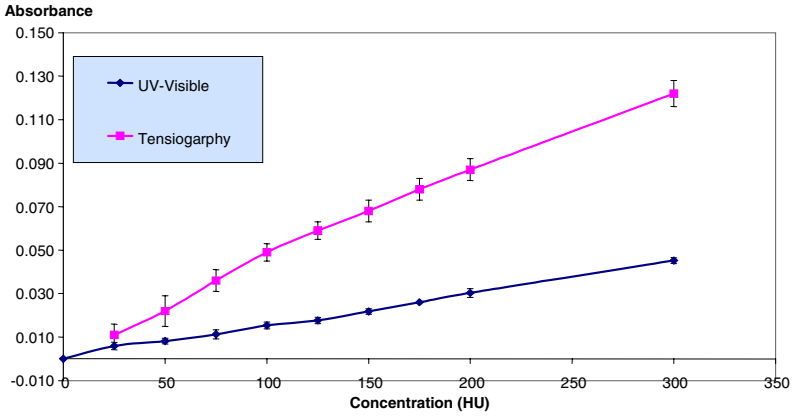

Figure 11. Comparison of UV–visible absorbance and tensiographic absorbance for colour standards at 470 nm in the concentration range 0–300 HU.

respectively, the rainbow and tensiopeak periods from a tensiotrace formed at any wavelength between 200 nm and 410 nm. Light intensity of 10% ethanol and acetaminophen concentrations were obtained from an acquisition point from (i) rainbow and (ii) tensiopeak period and both approaches delivered visually similar spectra. This qualitative result is interesting and can be extended in its implications. It informs us that any set of corresponding data from the same location in the tensiotrace can be used to produce spectra that will correspond to that obtained by a UV–visible spectrophotometer. Higher absorbance measurand sensitivity is seen here for the tensiopeak measurement, because this measurement is taken at a larger volume drop volume and hence a longer EPL than the rainbow peak measurement. This is not a general situation, as it is worth remembering that in some LUT such as alcohols, the rainbow peak is much greater than the tensiopeak. Measurement positions must be intelligently selected after giving proper consideration to the form of the tensiotrace.

The calibration absorbance–concentration graphs for measurements at both the rainbow and tensiopeaks were obtained from 10 data sets and as predicted from the drop spectroscopy equation have a greater slope for the tensiopeak having the larger EPL. This quantitative result also can be extended in its implications. It means that any data from a set of corresponding tensiotrace times could be used in quantitative drop spectroscopy. The penalty in using times that do not correspond to the peak maxima is a reduced sensitivity of the quantitative measurement.

The results of this experiment can thus be summarized simply that calibration graphs show an accurate linear dependences in which the error bars are too small to show on the graph. Consequently, equation (17) can be approximated to a first-order relationship, as the second-order correction factor is negligible. These are respectively

- For tensiopeak absorbance
  $A_{T_{\text{Tensiopeak}}} = 9 \times 10^{-5}\, C_t$ (correlation coefficient R for this fit $=1$). Here C_t is the concentration of the analyte.
- For rainbow peak absorbance
  $A_{T_{\text{Rainbow}}} = 6 \times 10^{-5}\, C_t$ ($R = 0.999$).

Here the tensiograph calibration sensitivities $\varepsilon T(\lambda, t)$ are, respectively, 9×10^{-5} and 6×10^{-5}. The tensiopeak sensitivity is 50% larger than the rainbow because of the longer EPL in the drop. The calibration sensitivity indeed here represents good instrument performance, considering that the concentration is measured in ppb.

There is one other factor worth a brief mention. The number of reflections producing the coupling in the drop at the rainbow peak is just two. The situation in the tensiopeak is more complex with an overlapping second order and third order at least both being present. It might be argued that the rainbow peak is a better measurement position because of this simpler optical coupling arrangement despite the fact that it usually has lower calibration sensitivity. However, in the view of the authors, such an advantage is only of marginal theoretical value; the real issue is the relative analytical sensitivities of a peak position.

4.3. Visible absorption and sensitivity analysis

The sensitivity of the drop spectrometer instrument has been investigated with a series of colour standards that were prepared as follows:1.246 g of potassium chlorplatinate and 1.000 g of cobalt (II) chloride hexahydrate were dissolved in 1 L of 0.1 M HCl to give a 500 HU stock solution [19]. The stock solution was diluted into seven aliquots with colour intensity ranging from 25 HU to 175 HU. A second set of standards was prepared to cover the range of 0 to 500 HU in increments of 100.

Ten replicate absorption readings of each standard were taken at 465 nm. The readings were made using a 1 cm cell in a UV–visible spectrophotometer (Varian Cary 1E). The average absorbance and standard deviation of the readings were calculated.

The solutions were tested with both the UV–visible spectrophotometer and the drop analyser. The standard method for colour determination is the platinum–cobalt (P–C) method [20] in which absorbance is taken at 465 nm. The centre wavelength of the LED used in the primary comparative study of sensitivity was 470 nm and therefore this source provides a good measurement for this P–C

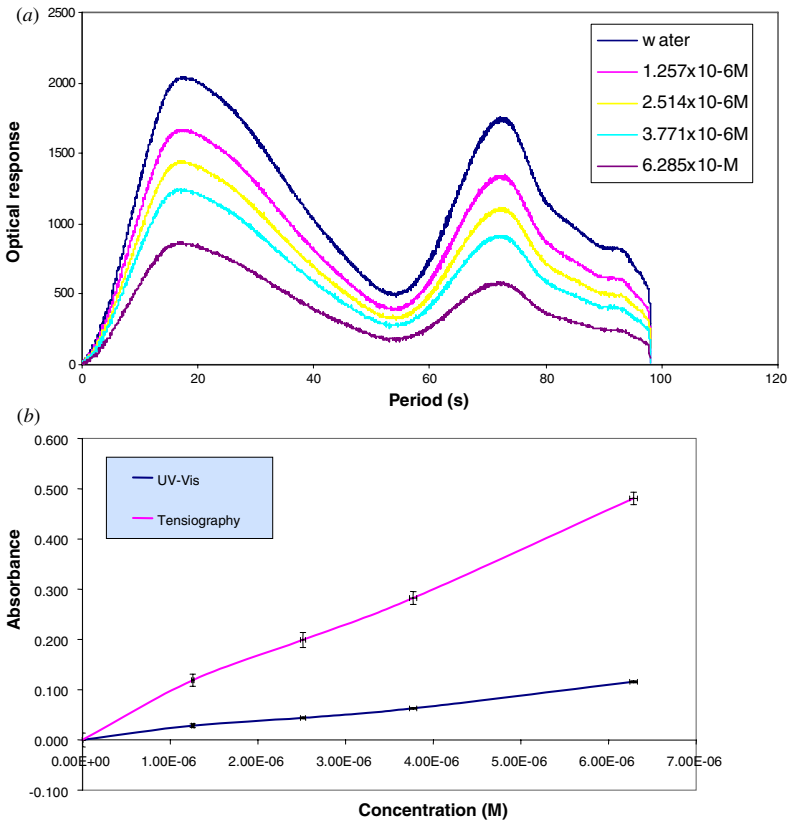

Figure 12. (*a*) Tensiotraces of FCF blue #1 solutions at 660 nm using PEEK drophead. (*b*) Comparison of UV–visible absorbance and tensiographic absorbance for Blue FCF at 660 nm in the concentration range 0–6.29 μM.

method. A comparison between the two methods is shown in figure 11.

The calibration sensitivity is of course the gradient of the UV–visible absorbance versus concentration graph and a value was obtained for the UV–visible spectrophotometer measurement of 1×10^{-4}. In the case of the drop spectrometer, the gradient was 4×10^{-4}. The drop instrument has four times the calibration sensitivity. The reason for this factor of 4 is one that requires some explanation, given that that the calibration sensitivity would be expected for drop analyser method to be about 1.5 times that of a standard instrument given that the EPL is approximately 1.5 cm at this measurement volume. This is a conundrum as there is no other apparent variability in these solutions that could account for an additional dependence on the analyte concentration, such as for example variations in refractive index with the analyte. The standard deviations of the measurand are larger for the drop analyser and therefore there is no noticeable analytical sensitivity (calibration sensitivity/standard deviation of the measurand) advantage here. However, since these results were obtained, instrumental modifications of the drop analyser have further reduced the measurand error and thus further improved the analytical sensitivity of the technique and the analytical sensitivity of the drop analyser is now comparable with that of the classical UV–visible.

The drop analyser data in figure 11 for the drop instrument were accurately fitted using equation (17) with the curve-fit passing through all the 3σ-error bars with the exception of the last data point. However, given that the fit-line intersects the error bar on the last data point, clearly the second-order fit is valid. However, these data sets are not of a sufficiently good standard to definitely prove the drop spectroscopy analytical–theoretical relationship of equation (17). Nevertheless, the curve-fitting study of these data does strongly support this theory. The first five data points in the calibration graph are accurately fitted with a first-order Beer's law relationship with EPL of about 10 mm, which is a result consistent with all experimental and modelling results. The absorption coefficient here obviously is not molar absorptivity, but in the standard concentration of colour solutions are given in Hazen units. The fit is 0.1068 HU^{-1} and all the data points in figure 11 are fitted with the second-order equation (17). The fitting dependence on this absorptivity value is very sensitive, as indeed is the fitting for the variance term, which is 0.0109 HU^{-1}. The latter fitting is quite specific as the best-fit value sits at the centre of a sharp valley and therefore the fitting error increases sharply as you move away from this best-fit value. Importantly, the fitting using equation (17) is 13.8 times better than can be achieved with a linear Beer's law fit.

Better sensitivity was obtained by tensiography than for standard UV–visible spectrophotometers in the analysis of the food colorant dye (FCF blue #1 (C.I./42096)). A comparison of calibration graphs for UV–visible and

Table 2. Summary of detection limits obtained by tensiography for the measurements of naphthalene and anthracene with the pulsed xenon source and continuous wave deuterium source.

	Tensiography		IRH
	Rainbow height detection limit (M)	Tensiograph peak height detection limit (M)	Detection limit (M) in IRH laboratory
Plused xenon source			
Naphthalene in de-ionized water	362×10^{-7}	8.1033×10^{-7}	4.5117×10^{-10}
Naphthalene is Volvic (mineral) water	1.258×10^{-6}	7.38×10^{-6}	Not measured
Naphthalene in tap water	1.3357×10^{-6}	9.629×10^{-7}	Not measured
Continuous wave deuterium source			
Naphthalene in de-ionized water	1.33×10^{-7}	1.33×10^{-7}	4.5117×10^{-10}
Anthracene in de-ionized water	4.3×10^{-8}	2.9×10^{-8}	1.683×10^{-10}

tensiographic absorbance is shown in figure 12. Again, the sensitivity is much higher for drop spectroscopy (respectively 76 877 and 18 006) delivering lower detection limits. One interesting and unexpected advantage of the drop spectrometer is that it appears that the upper limit of the dynamic range in the Beer's law analysis (marked by the departure from linearity where the sensitivity decreases) for the standard instrumental analysis may be lower in the drop analyser. The slope in drop spectrometer calibrations often shows an increase at higher concentrations, once again inexplicably showing an increasing sensitivity. Such somewhat idiosyncratic behaviour of course deserves some more detailed study in the future and some modelling studies are underway at this point to see if an explanation can be found.

A series of organic pollutants have also been used to compare the drop analyser and UV–visible spectrophotometer. The chemicals studied are herbicides, pesticides, PAHs (Polyaromatic hydrocarbons) and other organic molecules (e.g. atrazine, metabenzthiazuron, benzo a pyrene, anthracene, pentachlorophenol), which may be found in polluted waters. The usual method of analysis is via liquid chromatography or fluorescence. As a consequence of the presence of aromatic rings in these molecules, they strongly absorb in the UV region, but have very little absorbance in the visible range. These organic molecules do not absorb in the visible, and it was therefore necessary as in the acetaminophen study to use a drop analyser instrument working with a UV light source and a UV-CCD detector.

The most appropriate work to report here is for two of these priority organic pollutants that were analysed by tensiography at their wavelength of maximum absorbance. These were anthracene ($C_{14}H_{10}$) and naphthalene ($C_{10}H_8$). They are both PAHs (polyaromatic hydrocarbons) and both are found in industrial waters.

Although anthracene and naphthalene are not very soluble in water, because of their strongly absorbing properties, even trace amounts of these substances can be detected. The molecules have greater solubility in organic solvents such as alcohols and benzene. Here in the present study, methanol has been used to make up standard solutions for naphthalene, but anthracene solutions were prepared by making up water-based solutions. The solution was then filtered before being analysed with the drop analyser. The molarity of this sample was calculated from the calibration plot of a range of known concentrations of naphthalene and anthracene standards solutions in methanol, run on UV–visible spectroscopy at their λ_{max}. The tensiographic analysis was carried out at 220 nm and 252 nm and conducted using a pulsed xenon light source and a continuous wave deuterium source. In the drop analyser measurements, it was found that the pulsed xenon source gave poor repeatability between successive measurements, so the deuterium source was preferred as it is a continuous light source, giving good repeatability between measurements.

Tables 2 and 3 are of some importance to water monitoring applications. The Fifth Framework project Aqua-STEW (Surveillance Techniques for Early Warning (obviously of PAH and other pollution incidents)) was led by IRH who are authors in this paper. Simulated on-line and laboratory measurement programmes were undertaken as part of this project and one of the principal targets was some 20 priority pollutants (hereafter PP), and the conclusions drawn from the tables presented below for this study was that tensiography could measure many of these dangerous molecules at detection limits that made monitoring worthwhile. Associated data mining techniques were developed to provide the means to measure the target PP in real waters, which of course had a changing background of water quality. The full report is now with the commission [21] and further research reports are due to appear in due course to more fully detail the outcomes of this project.

4.4. Evaluation of the reproducibility of UV–visible spectrophotometry

An investigation was made into the reproducibility of UV–visible spectrophotometers with a view to providing the reasons for some of the improved performance characteristics of the drop analyser over the traditional cuvette instrument. A basic laboratory Shimadzu 460 UV–visible spectrophotometer was operated firstly at ambient temperature and then with temperature control. The ambient temperature study was made to determine the drift in the instrument when operated in a laboratory in which variable quantities of sunlight were incident on the instrument and can therefore be considered a worst-case situation. The investigation showed a drift of 12% (approximately 1.7% per hour) over a period of 7 h. In a second study, a Hitachi U-2000 UV–visible spectrophotometer

Table 3. Estimation of detection and quantification limits of 11 priority substances using the high-power xenon source coupled with the deep well spectrometer.

Substance	Fomula	Source	Detector	Estimated detection limit (M)	Estimated quantification limit (M)	IRH quantification limit (mg l^{-1})	IRH quantification limit (M)
Napthalene	$C_{10}H_8$	High-power xenon	S 1024 deep well	2.43×10^{-9}	8.09×10^{-9}	2.00×10^{-5}	1.55×10^{-10}
Anthracene	$C_{14}H_{10}$	High-power xenon	S 1024 deep well	2.11×10^{-8}	7.04×10^{-8}	1.00×10^{-5}	5.61×10^{-11}
Simazine	$C_7H_{12}N_5Cl$	High-power xenon	S 1024 deep well	4.16×10^{-9}	1.39×10^{-8}	3.00×10^{-4}	1.49×10^{-9}
Mecoprop	$C_{10}H_{11}O_3Cl$	High-power xenon	S 1024 deep well	1.26×10^{-7}	4.20×10^{-7}	5.00×10^{-5}	2.33×10^{-10}
Biphenyl	$C_{12}H_{10}$	High-power xenon	S 1024 deep well	4.58×10^{-8}	1.53×10^{-7}	5.00×10^{-5}	3.24×10^{-10}
Linuron	$C_9H_{10}N_2O_2Cl_2$	High-power xenon	S 1024 deep well	7.47×10^{-9}	2.49×10^{-8}	5.00×10^{-5}	3.24×10^{-10}
4-Octylphenol	$C_{14}H_{22}O$	High power xenon	S 1024 deep well	1.86×10^{-8}	6.18×10^{-8}	1.00×10^{-4}	4.85×10^{-10}
MCPA	$C_9H_9O_3Cl$	High-power xenon	S 1024 deep well	5.64×10^{-8}	1.88×10^{-7}	1.00×10^{-4}	4.99×10^{-10}
Atrazine	$C_8H_{14}N_5Cl$	High-power xenon	S 1024 deep well	4.94×10^{-8}	1.65×10^{-7}	3.00×10^{-5}	1.39×10^{-10}
Isoproturon	$C_{12}H_{18}N_2O$	High-power xenon	S 1024 deep well	1.73×10^{-8}	5.78×10^{-8}	5.00×10^{-5}	2.42×10^{-10}
Diuron	$C_9H_{10}N_2OCl_2$	High-power xenon	S 1024 deep well	9.28×10^{-9}	3.09×10^{-8}	3.00×10^{-5}	1.29×10^{-10}.

was tested and a drift of 7.2% (approximately 2.4% per hour) was observed over 3 h. The instrument was then thermostated and measurements were taken over 40 h. The temperature was initially 27 °C, but drifted to 27.5 °C over the test period. The absorbance readings in this time increased continuously and showed an overall 7.8% increase (approximately 0.2% per hour). The use of temperature control gave a very obvious improvement in the measurements.

Finally, a study was made of the error generated by the manual refilling of the cuvettes. This factor was investigated using the Hitachi instrument with temperature control. A standard error of 1.25% was obtained on a sample of 32 measurements. The test was repeated using a slider attachment for improved mechanical positioning of cuvettes. A standard error of 0.611% was obtained.

These simple tests seem to explain the improved performance seen for drop spectroscopy over the cuvette instrument. Drop delivery is highly reproducible under temperature control (the drop analyser is able to maintain the temperature to within an accuracy of 0.1 °C and reproducibility of 0.01 °C). The drophead is not touched in sample loading and automated sampling gives reproducible drop sizes. The observed drift of the UV–visible spectrophotometers, even when working in a differential dual beam mode, also demonstrated an important operational limitation. For standard UV–visible methods, the measurement procedure takes approximately 1 h. Within this time, the drift might be anything from 2.5% without temperature control to 0.2% with control.

5. Conclusions

This study has demonstrated some useful practical instrumental advantages of the drop analyser over the standard UV–visible spectrophotometer. The improved analytical reach of drop spectrometers could be important in some research fields. The technique with its quartz drophead can monitor/analyse LUT of any type, except hydrofluoric acid. Some discussion and experimental details have been provided on the relative sensitivities of the drop and standard UV–visible technique and there is little difference in measurement quality between the two techniques. Drop spectroscopy has a much greater dynamic range for absorbance measurements of up to 60 A units than the classical cuvette method with micro-drophead, simply because of the reduced path length.

The complexity of the tensiotrace (dependence on several properties of the LUT) makes it ideal for fingerprint applications of the simplest pass–fail variety and in such applications the sensitivity of the measurement can be tuned-down appropriately for any given application. Such reducing (dumbing down is perhaps a suitable term for this procedure) of the sensitivity is useful in beverage QA. Recently, an Enterprise Ireland Commercialisation Grant has been awarded to Carl Stuart Ltd [22] to develop for a leading brewing company a fingerprint system that will be based on a reduced sensitivity drop analyser monitor. The aim is to provide a total-product quality assurance system.

A 3D ray-tracing model has been developed and tested in successful investigations into some real water applications for the Fifth Framework Aqua-STEW Project. Although this work is not detailed here, this study demonstrated the theoretical possibility of tensiographic differentiation of coloured and turbid solutions. It appears that the drop analyser can offer both qualitatively and quantitatively spectroscopic differentiation between liquids. An analytical theory of drop spectroscopy has been developed and presented here for the first time. This theory has been tested against experiment including some detailed enquiries into the average EPL. The best technique for quantitative drop spectrometer measurement has been determined by a statistical theoretical enquiry and the result established by experiment. The performance of the drop spectrometer has been evaluated against a number of traditional types of modern spectrophotometers, with measurements provided in this study by an internationally accredited standards laboratory (Starna) working with a Carey instrument. In a series of trials here and elsewhere, the drop analyser has shown some comparable detection limit and sensitivity to the classical technique, for example, in priority pollutants measured in real waters. Experimental evidence

of micro-errors in absorbance measurements from traditional cuvette placement has been suggested as one contributory shortcoming in traditional instruments. For whatever reason, it is an important finding that drop spectroscopy generally delivers comparable, or indeed improved, detection limits to the traditional temperature controlled spectrometers. The technique has also been shown to be useful in research pharmaceutical applications. Although not detailed here, the technique has been applied to many other areas of applications.

The fact that the fibre drophead system does not provide a constant EPL is at first sight an overwhelming a disadvantage. However, it is well known that there are measurement problems associated with cuvettes. Errors in mechanical construction and collimation mean that a standard path length is only really true at a theoretical level in traditional UV–visible spectrophotometry. It has been shown here that average path length for solutions can be determined accurately (providing certain physical characteristics of the liquid are known) for the drop analyser using either the experimental or computational methods described in this work. This study has shown that although drop spectroscopy is most obviously a departure in this established technique, there are many applications where the improved performance and the advantages of microvolume samples count. The ease of cleaning a quartz drophead indeed makes automation much simpler than with even flow-through cells in traditional instruments. The temperature control of the drop analyser also offers better system reproducibility than can be obtained with cuvettes as the repositioning error of the cuvette has shown to be the major performance-limiting factor in this regard for established instruments.

This paper provides indications to the quantification of measurement potential of both LED-photodetector and CCD/CMOS drop spectrometer instruments. There have been some significant recent developments principally in the field of sessile drop spectrophotometry. The major commercial development since 2000 by Nanodrop Corporation [23] has produced a growth of micro-volume spectrophotometer/fluorimeter applications. These instruments are, however, not true drop spectrometers/fluorimeters, but are rather mechanical contrivances which make the micro-volume measurement after placing a drop on an anvil that then draws up a capillary of liquid required for this measurement [24]. The approach we describe here has been adapted for measurements of 1 μL volumes and with sessile drops and a 1.5 mm EPL is obtained, which represents an improvement of 50% on the Nanodrop instrument. With the pendant drop measurements we can obtain EPLs that are much more than an order of magnitude greater than the Nanodrop instrument and the spectrometer is self-cleaning as it is made of quartz that protect the fibres from contamination. The sessile-drop spectroscopy microvolume approach has an improved sensitivity over the other approach that the increased volumes required for the analysis is easily catered for by dilution. This dilution is of course a major disadvantage for the pendant drop spectrometer over that of the sessile drop spectrophotometer. The theoretical analysis described here, although for pendant drops, applies to these microvolume sessile-drop spectrometers.

Finally, it is worth pointing out in conclusion that all the measurements reported here were done on an old version of the drop analyser and the new system has radically improved signal-to-noise over this old instrument. This instrumental advance will have a major impact on the detection limits possible and we are confidently projecting in the forthcoming tests detection limits of 10 pM or lower. Recent work by M O'Neill and M Perrugot has shown that a drop theory applies to sessile drops that are placed on a drophead by a microvolume pipette. This work shows that the technique described here can be scaled down and deliver the spectroscopic measurement of concentration of analyte. An extended experimental study has shown that the best way to make drop absorbance measurements is signal averaging at the tensiopeak. The discovery of a simple linear experimental relationship between drop period and tensiopeak period is something therefore which impacts on microvolume drop spectroscopy, except it does mean that the measurement volume is known for the LUT, because the tensiopeak in all practical situations with water-based solutions gives the maximum peak position. In alcohols, the rainbow peak must be used as the tensiopeak is much reduced. A further factor to be considered is the EPL and in strongly absorbing solutions it may be prudent to use the rainbow peak as this corresponds to a shorter EPL and hence could extend the dynamic range of the absorbance measurement. The importance of this discovery goes well beyond these present spectroscopic issues as it has implications for surface protein science in the classical drop volume method and will be the subject of another paper.

Acknowledgments

The financial support by the Deutsche Forschungsgemeinschaft (grant Pi 165/12-1) for N Wüstneck and R Wüstneck is gratefully acknowledged, and the personal encouragement from Austin Duke played an important part in the development of this project.

References

[1] McMillan N D *et al* 2008 Tensiograph platform for optical measurements: theoretical, experimentally-referenced and software for measurement and monitoring/fingerprinting applications *Drops and Bubbles in Interface Science*, *Studies in Interface Science* ed D Möbius and R Miller (Amsterdam: Elsevier)

[2] McMillan N D, Finlayson O, Fortune F, Fingleton M, Daley D, Townsend D, McMillan D and Dalton M 1992 The fiber drop analyser: a new multi-measurand analyser with applications in sugar processing and for the analysis of pure liquids *Meas. Sci. Technol.* **3** 746–64

[3] O'Neill M, McMillan N D, Smith S R P, Hammond J P, Smith S and Hulme K 2007 New versatile approach to microvolume drop spectroscopy: instrumental innovation and testing for UV-calibration and DNA standards *Int. Workshop: Drops and Bubbles Interfaces, Grenada, Spain* Poster P 42

[4] Bertho A C, McMillan D D G, McMillan N D, Smith S R P and O'Rourke B 2005 Optical studies into the SPLITS effect: new insights into controlling sampling errors in turbid solutions for analytical instruments *Proc. SPIE* **5826** 99–109

[5] Riedel S 2007 Developments in tensiographic multivariate analysis leading to a new approach with prevalent

applicability for sample fingerprinting and data representation (Kingston University, Surrey)
[6] Harkins W D and Brown F E 1919 The determination of the surface tension (free surface energy) and the weight of falling drops: the surface tension of water and benzene by the capillary height method *J. Am. Chem. Soc.* **41** 449–503
[7] Yildirim O E, Xu Q and Basaram O A 2005 Analysis of the drop weight method *Phys. Fluids* **17** 062107
[8] Morrin D, McMillan N D, O'Rourke B, Smith S R P, Pringuet P and O'Neill M 2008 An important new empirical relationship between drop period and tensiopeak period with surface measurement applications, in preparation
[9] Tiernan K, Kennedy D and McMillan N D 2005 Tensiograph instrumentation for measuring liquid material properties *Mater. Des.* **26** 197–201
[10] McMillan N D, Davern P, Lawlor V, Baker M, Thompson K, Hanrahan J, Davis M and Harkin J 1996 The instrumental engineering of a polymer fiber drop analyser for both quantitative and qualitative analysis with special reference to fingerprinting liquids *Colloids Surf.* A **114** 75–97
[11] Tiernan K 2008 Drop spectrophotometer design *PhD Thesis* (DIT, Dublin)
[12] Carbery D, Riedel S M and McMillan N D 2001 An experimental investigation into the engineering basis of a new fiber optic small volume drop surface analyser *Sensors and their Applications XI* (Bristol: Institute of Physics Publishing) pp 209–14
[13] McMillan N D, Finlayson O, Fortune F, Fingelton M, Daly D, Townsend D, McMillan D D G, Dalton M J and Cryan C 1992 A fiber drop analyser: A new analytical instrument for the individual, sequential, or collective measurement of the physical and chemical properties of a liquid *Rev. Sci. Instrum.* **63** 216–27
[14] Gerhardt C 1853 Untersuchungen über die wasserfreien organischen Säuren *Ann. Chem.* **67** 149
[15] Clarke E C G 1969 *Isolation and Identification of Drugs* (London: The Pharmaceutical Press)
[16] Donç E and Baleanu D 2002 Two new spectrophotometric approaches to the multicomponent analysis of the acetaminophen and caffeine in tablets by classical least-squares and principal component regression techniques *Il Farmaco* **57** 33–7
[17] Clarke E C G 1969 *Isolation and Identification of Drugs* (London: The Pharmaceutical Press)
[18] Morrin D 2007 *Experimental Studies in Tensiography PhD Thesis* (Carlow: Institute of Technology)
[19] *US Standard Methods for the Examination of Water and Wastewater* 1995 19th edn (APHA)
[20] Method 10068, Hach DR/2010 Spectrophotometer Handbook
[21] Full Evaluation Report 283 EU 5th Framework Project 2004 Aqua-STEW (Development of Optical Sensing Techniques for Water Quality Determination)
[22] Enterprise Ireland Commercialisation Grant 2007 Development of a stand alone multifunctional laboratory accredited beverage analyser monitoring system for the beer manufacturing process Project No 139030|RR
[23] Nanodrop patents are US 6,628,382 B2 (Sept 2003) and US 6,809,826 B2 (Oct 2004)
[24] McMillan N D, Smith S, O'Neill M and Baker M Microvolume spectrophotometer *Irish Provisional Patent* filed 12 May 2006 S2006/0381